Contents list available at CBIORE journal website

International Journal of Renewable Energy Development

Journal homepage: https://ijred.cbiore.id

Research Article

A systematic decision-making approach to optimizing microgrid energy sources in rural areas through diesel generator operation and techno-economic analysis: A case study of Baron Technopark in Indonesia

Adinda Prawitasari[a*], Vetri Nurliyanti[a], Dannya Maharani Putri Utami[a], Eka Nurdiana[a], Kholid Akhmad[a], Prasetyo Aji[a], Suhraeni Syafei[a], Ifanda[a], Iwa Garniwa Mulyana[b]

[a]*Research Center for Energy Conversion and Conservation, National Research and Innovation Agency, Serpong, Indonesia*

[b]*Electrical Engineering Department, Faculty of Engineering, Universitas Indonesia, Depok, Indonesia*

Abstract. Microgrid systems are part of the most reliable energy supply technologies for rural communities that do not have access to electricity but the system is generally dominated by diesel generators (DG). The implementation of de-dieselization programs to ensure efficient diesel operations requires addressing several scenarios such as the replacement of diesel completely with 100% renewable energy sources at a significant cost. The design and selection of appropriate configuration, as well as operating patterns, need to be considered in adopting economical and reliable microgrid systems. Therefore, this study aimed to design an optimal configuration and operational pattern for microgrid systems for the frontier, outermost, and least developed (3T) regions using Baron Techno Park (BTP) in Indonesia as a case study. The optimization was conducted through HOMER software combined with benefit-cost analysis and the focus was on daily load variations, selection of control algorithms, reconfiguration of the power supply system, and setting of the diesel generator operating hours. The results showed that the optimum configuration was achieved using loads of resort, 24 kWp of PV, 288 kWh of BESS, load-following (LF) as dispatch controller, and 25 kVa of DG. Moreover, the proposed microgrid system produced 12% excess energy, 36% renewable fraction (RF), 13.25 tons reduction in CO_2 emissions per year, $0.28 LCOE per kWh, $250,478 NPC, and a benefit-cost ratio (BCR) of 0.89. It also had a potential energy efficiency savings of 55.56% and a cost efficiency of 20.95% compared to existing system configurations. In conclusion, the study showed that the addition of DG to microgrid systems in 3T areas was more optimal than using only PV and batteries. An effective operating schedule for the DG was also necessary to improve RF and reduce expenses. Furthermore, other energy storage devices considered less expensive than batteries could be introduced to improve the economics of microgrid systems in the 3T region.

Keywords: Benefit-cost ratio, Cost efficiency, Diesel generator operation, Excess energy, Microgrid optimization, Renewable fraction.

Received: 10th Nov 2023; Revised: 18th January 2024; Accepted: 22nd February 2024; Available online: 25th February 2024

1. Introduction

The CO_2 emissions from the combustion of fossil fuels in power plants are classified into three main target categories of the energy sector based on the IPCC Guidelines 2006 (Intergovernmental Panel on Climate Change, 2006). Indonesia has implemented a strategy to reduce greenhouse gas emissions nationally by 29% in 2030 with a focus on the decrease of 91.74 million tons of CO_2 equivalent in the energy sector (Direktorat Jenderal Pengendalian Perubahan Iklim, 2017). Moreover, the diminishing fossil fuel reserves have led to the introduction of renewable energy sources as an alternative solution. The purpose of these initiatives is to reduce the environmental harm caused by the combustion of fossil fuels. This has led to the development of microgrid systems using renewable energy sources close to consumers in order to reduce the need for significant transmission lines and associated losses. However, the systems using renewable sources as the main energy have certain drawbacks such as intermittence in power output. The problems identified showed there was the need to apply different forms of optimization processes. This has led to the implementation of demand-side energy management strategies for residential and commercial load profiles to provide a better solution for maximizing renewable energy (Bhamidi & Sivasubramani, 2020; Martirano *et al.,* 2019).

A microgrid system can be designed through two control architectures which are centralized and decentralized. In a centralized architecture, there is a centralized controller to collect data and information such as power generation sources, meteorological data, and load profiles as well as determine optimal energy usage. It has the ability to supply active and reactive power according to predefined setpoints using Virtual Synchronous Machine (Jmii *et al.,* 2020). Meanwhile, the decentralized architecture is the distribution of control functions across multiple components or subsystems within the

* Corresponding author
Email: adino05@brin.go.id (A. Prawitasari)

https://doi.org/10.61435/ijred.2024.59560
ISSN: 2252-4940/© 2024.The Author(s). Published by CBIORE

microgrid, allowing for autonomous operation and coordination without reliance on a central controller. Based on the increasing integration of renewable energy resources in microgrid control systems, this architecture requires multifunctional converters that can enhance the interaction between power sources, loads, and storage (Liu & Liu, 2019). Furthermore, a microgrid energy management strategy designed to save fossil fuels and lower CO_2 emissions focuses on using renewable energy and battery capacity as the primary source and a diesel generator as the backup (Anglani *et al.,* 2017). The dispatch control strategy to monitor the operation of renewable energy generators, diesel generators (DG), and storage devices is the cycle charging (CC) and load-following (LF) methods (Ishraque *et al*., 2021),(Jahangir *et al.,* 2023). The combination of these generation sources to smooth out load patterns in a hybrid power generation system can be achieved by adding a battery as energy storage (Sulistyo & Far, 2020). Therefore, when there is an excess of renewable energy sources, the energy storage batteries can be charged without using a diesel generator (Azahra *et al.,* 2020). Moreover, the development of renewable energy-based power generation systems, such as hybrid or microgrid systems with batteries or DG, can be expanded to ensure power reliability and provide 24-hour electricity supply to the frontier, outermost, and least developed (3T) areas (PT PLN, 2021).

The optimization of renewable energy systems requires identifying potential local energy resources to be implemented in order to meet the surrounding load demands. Moreover, the consideration of economic and environmental criteria with the high solar irradiance for 3T areas requires using a hybrid system that combines solar energy, a diesel generator, and batteries (Yaouba *et al.,* 2022)(Dei & Batjargal, 2022). The design of an islanded hybrid microgrid with wind turbines, solar modules, a diesel generator, and battery storage based on LF control strategies has been identified as part of several strategies to achieve the lowest values for LCOE, NPC, and CO_2 (Ishraque *et al*., 2021; Jahangir *et al.,* 2023).

The Indonesian government, through Presidential Regulation No. 63 of 2020, established criteria for identifying disadvantaged areas based on six factors including community economy, human resources, infrastructure, regional financial capacity, accessibility, and regional characteristics (Kemeterian Sekretariat Negara Republik Indonesia, 2020). According to these criteria, 62 regencies in Indonesia are classified as disadvantaged areas, with a national rural electrification ratio of 99.79%. The areas include 107 locations with access to 24-hour electricity as well as 236 without access (Dirjen Ketenagalistrikan ESDM, 2023). The government is developing local renewable energy sources and optimizing energy resources, load management, and power generation operations to improve the rural electrification ratio, specifically in the 3T regions, where grid expansion is not feasible due to various challenges. Meanwhile, the de-dieselization program implemented to improve electrification, particularly in the 62 disadvantaged, remote, and frontier areas (Kementerian Sekretariat Negara Republik Indonesia, 2020), requires DG as a backup power sources (Anglani *et al.,* 2017). Therefore, this study aimed to optimize the existing microgrid system by maximizing the utilization of renewable energy resources and power generation operations.

The study area was the Baron Tekno Park (BTP) which was designed to explicitly target the 3T regions. The National Research and Innovation Agency of Indonesia has been managing BTP since its creation by the Agency for the Assessment and Application of Technology in 2010. It serves as a research, development, and distribution center for renewable energy technology. The BTP area, located in Gunung Kidul Regency, Yogyakarta Special Region, was selected for this study due to the significant potential for renewable energy resources. The facility functions as a central hub for conducting research, engaging in development activities, and providing training opportunities in the field of renewable energy technology. It also serves as a prominent destination for science and technology tourism, particularly concerning the exploration of novel renewable energy solutions. A solar energy system with a capacity of 36 kWp is used to power all the activities conducted within the BTP area. There are also other alternative energy sources within the vicinity, such as wind energy and DG.

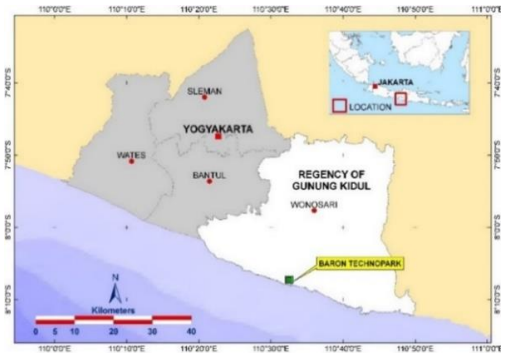

Fig 1 Baron Technopark Location.

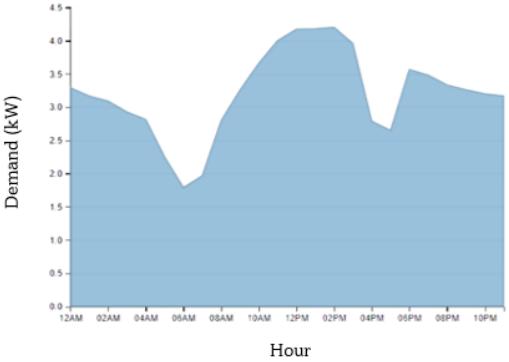

Fig 2 Daily load profile of BTP

The focus of this study was to optimize the existing microgrid system during the operational stage. This was accomplished by using the existing wind energy turbines and fossil fuel generators previously applied as the backup power. The process led to the improvement and establishment of the existing system components as the baseline configuration. Furthermore, load patterns were included to increase energy efficiency and expand the capabilities of the system. This showed that the aim of the proposed system was to maximize the use of renewable energy sources while minimizing surplus energy production and considering other relevant economic factors. The main aim was to enhance the energy efficiency and economics of the microgrid system.

2. Method

2.1. Overview of the Current Microgrid System in the BTP

2.1.1. Location and Daily Load of the BTP

BTP is a 9.25-hectare area located in Gunung Kidul Regency, Yogyakarta, as presented in Fig 1. It is situated near the coastline and can be found at the coordinates of latitude -8.132 and

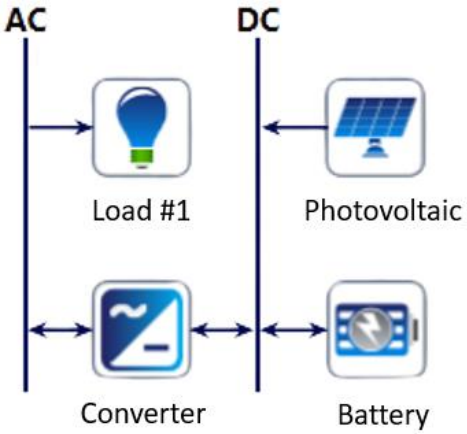

Fig 3 Schematic of Existing BTP microgrid system.

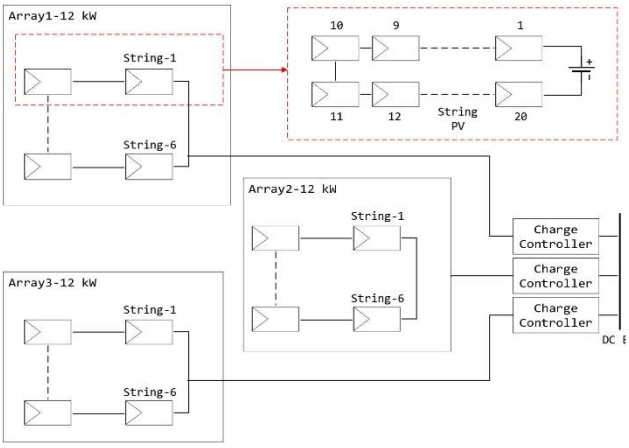

Fig 4. Configuration of the 36 kWp PV array at the BTP

Fig 5 BESS setup in the BTP.

longitude 110.544. The area has several structures, including a central facility, an administration center, a security checkpoint, and employee accommodations. The buildings are equipped with lighting, air conditioning, and different electrical appliances, which constitute a daily energy demand with a load profile, as shown in Figure 2. Photovoltaic (PV) system installations and battery storage systems are installed to power these buildings through the AC/DC coupling converters presented in the schematic of Figure 3. Meanwhile, there is a considerable burden on the BTP supplied by the diesel generator (DG) which is in the form of the water pump used for the Sea Water Reverse Osmosis (SWRO) and Brackish Water Reversed Osmose (BWR) systems as non-drinkable water consumption.

2.1.2 PV system configuration

The PV system converts the energy from sunlight in photons directly into electricity (Khamharnphol *et al.,* 2023). However, the electrical power generated by the conversion significantly depends on several factors, including cell structure, cell, and ambient temperature, temperature coefficient, derating factor, solar radiation, as well as the environmental and meteorological conditions at the installation site (Çetinbaş *et al.,* 2019) The implementation of PV systems in coastal areas has several advantages and challenges. The main advantage is the high rainfall levels of the area which often assist in cleaning the surface of the solar panels to produce more output power. Meanwhile, the challenges range from climate change, the resistance of solar panels (Emetere *et al.,* 2016), and the abundance of cloud movements causing atmospheric shading (Emetere & Akinyemi, 2015).

The BTP is equipped with a 36 kWp PV array that uses a 100 Wp polycrystalline type module at an efficiency of 14%. The PV system is configured into 3 arrays of 12 kWp each containing 6 strings, leading to a total of 18 strings. Moreover, each of these strings consists of 20 PV modules connected in series as observed in the configuration diagram presented in Figure 4. A PV output voltage of about 360 V is produced through the system which is subsequently connected to an inverter with a capacity of 25 kW. The choice of this capacity is due to the consideration of power the PV arrays and loads can produce. In this simulation, PV arrays were assumed to have a lifetime of 25 years, the cost was based on the findings of Chisale et al. (2023), and the derating factor was set at 85% (Beza *et al.,* 2021).

2.1.3 Battery Energy Storage System (BESS)

The storage of energy in batteries can improve the reliability of microgrid systems to address the intermittent challenges of renewable energy generation. Moreover, several control strategies in BESS were reported to have the capacity to lower LCOE values in addition to optimal energy storage for small-scale isolated hybrid renewable energy systems (Jufri *et al.,* 2021a). A lead acid battery produced by the Shoto brand GFX-1200 with a voltage specification of 2V and a capacity of 1200 Ah is used in the microgrid system at the BTP, as shown in Figure 5. Furthermore, a total of 120 units of batteries, connected in series to produce an output voltage of 240V, are installed and the cost of each is estimated in Thirugnanam *et al.* (2018).

2.1.4 Inverter

The inverter used in the BTP is a three-phase bidirectional dual-mode hybrid converter for microgrid systems. It can be used for some types of renewable energy sources, such as PV, wind turbines, and micro-hydro combined with diesel generators (DG) both on DC and AC connections. Several studies applied this type of inverter in the configuration of microgrids in remote areas due to its reliability (Mudaheranwa *et al.,* 2023; See *et al.,* 2022; Upadhyay & Sharma, 2016; Yaouba *et al.,* 2022). The specific type used in this study was the Leonics Apollo MTP-413F with a capacity of 25 kW which was selected

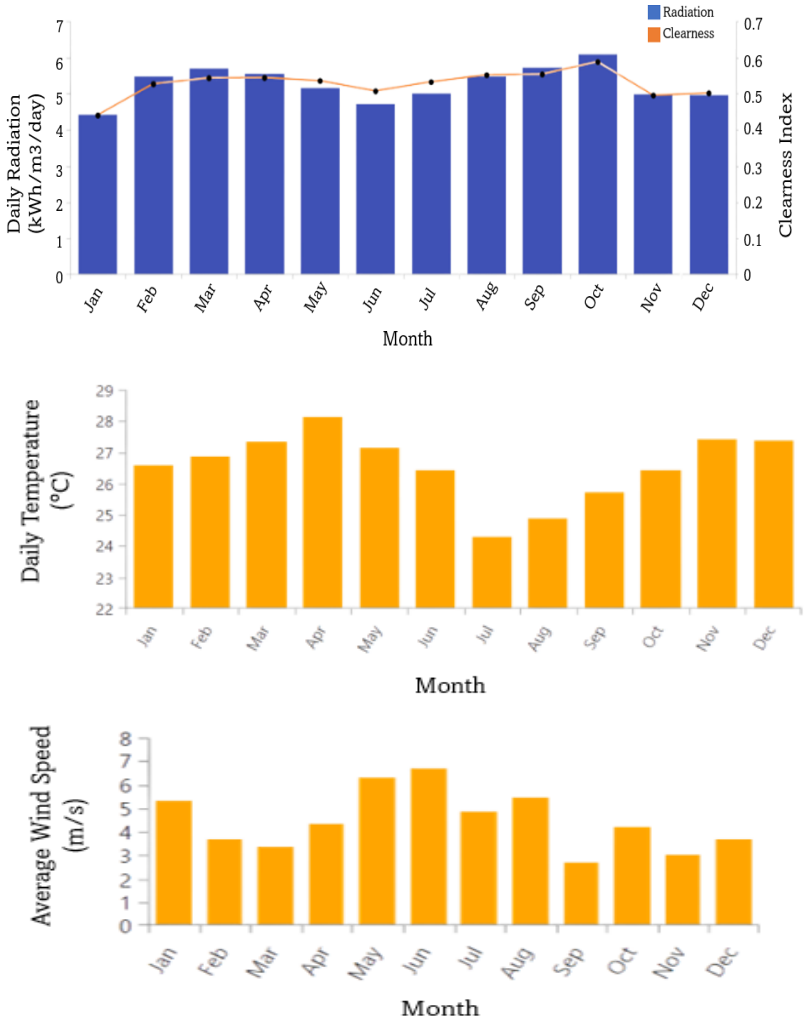

Fig 6. Baron Techno Park (a) Solar Global Horizontal Insolation. (b) Ambient Temperature Data. (c) The wind speed potential.

based on the DC to AC power capacity ratio (Díaz-Bello *et al.*, 2023). This was due to the fact that the maximum AC power output of the inverter was the energy to be used by the entire hybrid system.

2.2. Energy resources

Sensor devices were deployed at the BTP location to monitor the current state of the available resources and the data collected were transformed into 8,760 hours per year to be used in the simulations. The dataset focused on global horizontal irradiance (GHI) with an annual average insolation of 5.27 kWh/m²/day in Figure 6 (a), ambient temperature of 26.74 °C in Figure 6 (b), and ambient wind speed with 4.23 m/s in Figure 6 (c),

2.3. Optimization methods

The initial phase of this study was the collection of data and information on previously installed microgrid systems to have an insight into the operational circumstances and performance. The data on the components, load profiles, configuration, and operation were used as an input while the potential data on renewable energy sources such as solar irradiation intensity and wind speeds were included in the initial data collection process. Subsequently, the performance of the existing was determined using HOMER based on the measurement and simulation results. During the simulation, the components were pre-

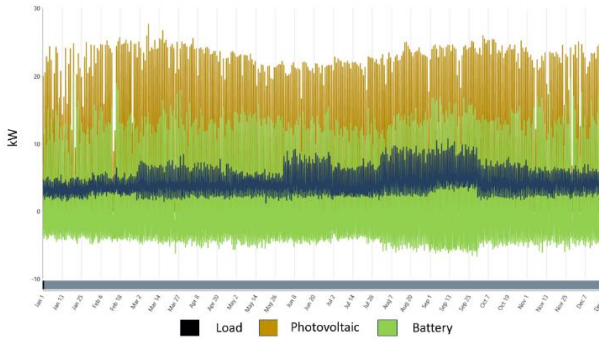

Fig 7. Aggregate power sources from the existing system for a year.

installed and this led to the exclusion of the investment cost from the consideration. The costs considered include replacement, operating, and maintenance (O&M) as well as other additional simulation parameters listed in Table 1.

2.3.1 Analyzing the present state of the system

The microgrid system implemented at the BTP was designed using PV and batteries for energy storage. Meanwhile, the existing system was evaluated to determine the aggregate

Table 1
Simulation input parameter

Parameter	Specification
Economics	
Nominal discount rate	5.75%
Expected inflation rate	3.52%
Project Design	
Project lifetime	15 years
Minimum renewable fraction	10%
Photovoltaic	
Replacement	$573
O&M	$1/years
Lifetime	25 years
Battery	
Replacement	$255
O&M	$51/years
Lifetime	8 years
Inverter	
Replacement	$4806
O&M	-
Lifetime	10 years
Wind Generator	
Replacement	$9234
O&M	$159/year
Lifetime Lifetime	20 years
Diesel Generator	
Replacement	$2229
O&M	$1/years
Lifetime	15.000 hrs
Benefit Cost Ratio	
Emission factor	0.53 kg/kWh
Carbon tax rate	$0.0019
Renewable Energy Certificate	$2.23

energy produced to fulfill daily demands. This was achieved by analyzing simulation results obtained through HOMER software using operational data collected for one year as input as presented in Figure 7. The calculations were conducted using a derating factor of 85% and this led to a maximum solar energy production of 30 kWp from the overall installed PV capacity of 36 kWp.

The next step was to compare the two systems, specifically looking at how the direct measurements of the existing system were processed compared to the HOMER simulation. A striking similarity was observed between the variables in Table 2 which was used to show the complete analysis of power demand, power output from solar sources, and excess energy. Consequently, the HOMER simulation was selected for this study.

Excess energy was defined as the energy not used by the load and could not be stored in the batteries, as presented in Fig 7 for June and September. These months had reduced surplus energy due to heightened demand compared to the other months. Moreover, the exclusive usage of PV and BESS components was attributed to the low load and this led to the underutilization of other generating components in the system.

Table 2
Comparison of measurement results and simulation for the BTP existing system

Parameter	Measurement Results	HOMER Simulation
Energy Demand (kWh/year)	36.544	36.510
Annual PV Production (kWh/year)	45.605	55.394
Excess Energy (%)	20	27

To accommodate increased demand in the BTP area, optimization efforts were applied to the existing components, such as wind generators and DG. The focus was to incorporate additional loads and use supplementary generators.

The energy architecture of the BTP explored the advantage provided by the presence of other generator components in the area. The existing setup, which included adding extra generators, was designated as the baseline configuration, as shown in Table 3. The two configuration systems had a reduced net present cost (NPC), levelized cost of energy (LCOE), and benefit-cost ratio (BCR). However, the initial proportion of renewable energy was reduced from 100% to 25% in the baseline configuration and the first surplus energy of 27% increased to 56%. This was used as the foundation for the optimization process through the application of the components accessible within the specified region.

2.3.2 Optimization scheme

The method implemented in this study to optimize energy was based on the consideration of the daily loads, energy

Table 3
Configuration of the Power Generation System.

Parameter	Existing Configuration	Baseline Configuration
Photovoltaic	36 kWp	36 kWp
Wind Generator	-	5 kW
Diesel Generator	-	20 kW
BESS	288 kWh	288 kWh
NPC	$258046	$189027
LCOE	$ 0.56	$ 0.41
Renewable Fraction	100%	25%
Excess Energy	27%	56%
BCR	0.735	0.445

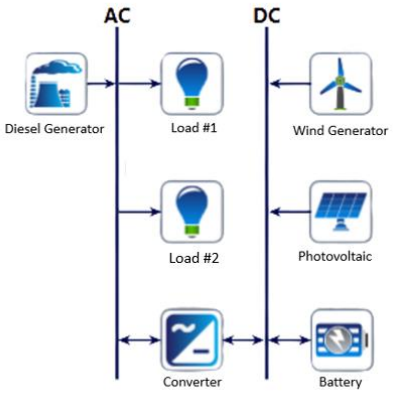

Fig 8. Optimizing the microgrid system schematic by incorporating added loads, power sources, and scheduled generator operation.

sources provided, and changes in the operating hours of the fossil fuel generator. The primary components of the initial setup solely consisted of solar panels and BESS. Meanwhile, the optimization simulation added a wind generator (WG) and a diesel generator (DG) to the proposed baseline schematic system architecture, as shown in Fig 8. The objective was to minimize costs and mitigate losses from the production of surplus energy.

The microgrid generator operation and consideration of the uncertainty of energy sources across different load was optimized to achieve effective cost reduction (Hou *et al.,* 2023). Moreover, the choice of the controller algorithm was a factor considered throughout the optimization process. The HOMER simulation used also had three distinct controller algorithms, including cycle charging (CC), load-following (LF), and combined dispatch (CD).

The simulation results were evaluated to identify the effect of different optimization schemes or scenarios implemented on excess energy, renewable energy factors, and cost parameters including total annual and levelized energy costs. Moreover, the configuration of the proposed system was selected and analyzed based on some optimization objectives and limitations, as presented in Table 4. The most optimal system was later determined by evaluating the cost-effectiveness and potential for energy savings. The cost savings were determined through the evaluation of benefit-cost ratios while the energy savings were assessed by comparing the excess energy values of each proposed system with the existing and the baseline.

The optimization process was assessed in terms of the LCOE, NPC, and renewable fraction (RF) (Dahiru & Tan, 2020). The

Table 4
Optimizing Parameters

Optimization criteria	Constraints
Criteria 1 (Minimum NPC)	NPC < existing system
Criteria 2 (Minimum LCOE)	LCOE < existing system
Criteria 3 (Maximum RF)	RF > baseline system
Criteria 4 (Minimum excess energy)	Excess energy < existing system
Criteria 5 (Maximum Benefit Cost Ratio)	-

NPC is an essential project metric in a generation system that focuses on a range of expenditures, including those expended on installation, maintenance, operation, and replacement of components during the duration of the project. Equation 1 formally defines the variable *Ct*, denoting the total annual expenditure accrued throughout a specific period of *t* years for a given investment. The variable *n* represents the whole time associated with the existence of the project and *r* signifies the annual discount rate.

$$NPC = \sum_{t=1}^{n} \frac{C_t}{(1+r)^t} \quad (1)$$

The determination of the average cost of producing electricity per kilowatt-hour (kWh) is an important method to evaluate the technological and economic aspects of a power generation system. The average cost was computed using the formula in Equation 2, where, C_G, C_B, H_S, and E_S represent the annual cost of electricity generation, total marginal cost of boilers, total heat provided, and total electricity provided, respectively.

$$\text{LCOE} = \frac{C_G - C_B H_S}{E_S} \quad (2)$$

The contribution of renewable generators to the total energy was calculated in this study using Equation 3. The renewable fraction value (f_{RF}), energy from non-renewable sources (E_{DG}), and the total energy fulfilled (E_{ES}) were considered.

$$f_{RF} = 1 - \frac{E_{DG}}{E_{ES}} \quad (3)$$

1) Optimization of Daily Load Addition

Load requirements can be ascertained during a specific period and classified into several categories including primary,

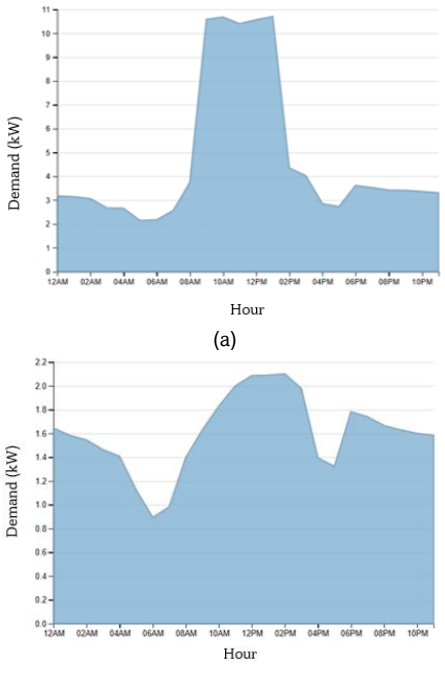

Fig 9. Energy (a) Load B: Combined daily load of the BTP and SWRO/BWRO. (b) Load C: Daily load of a resort.

Table 5
The mean load for each setup.

Metric	Load A	Load B	Load C
Average (kWh/day)	102.12	129.89	160.57
Average (kW)	4.25	5.41	6.69
Peak(kW)	10.93	23.31	33.89

deferrable, thermal, and hydrogen loads within the context of modeling. Moreover, the requirements can be expressed in the form of a load profile which is in different classes such as residential, commercial, industrial, or community load profiles. The optimization modeling used was established on the load requirements presented in Fig 9 (a) and (b). More precisely, the principal load used was accompanied by a commercial load profile.

The addition of a water treatment system powered by diesel energy was part of the change proposed to the baseline configuration in order to maximize the benefits of producing extra energy. Moreover, the load was increased during the daytime when the PV energy produced by the system was at its peak, typically between 10:00 a.m. and 2:00 p.m. as presented in Fig 9 (a). The energy was to fulfil the requirements of the water treatment system, specifically a 10.7 kW SWRO system, during four months consisting of June, July, August, and September. Furthermore, a 6.4-kilowatt brackish water reverse osmosis (BWRO) water treatment plant was used throughout different months of the calendar year. It was important to state that the common term used to describe the extra burden in this study was “Load B”.

An alternative arrangement to integrate daily loads was to include the daily resort loads, as presented in Fig 9 (b). The development plan of the resort was assumed to require 50% of the initial daily load of the BTP alongside the SWRO/BWRO system. The term used to describe the extra burden was "Load C" as presented in Table 5 describing Load A, Load B, and Load C.

2) Optimization of power generation system configuration

The existing energy sources in the BTP can be harnessed to fulfill the growing electricity demand outlined in the development plan. Therefore, alternative energy sources, including wind and DG, were included as supplementary choices in the optimization simulation setting.

The physical setting of the BTP area was characterized by the placement in a coastal region with rocky terrain and position at an elevation of 20 meters relative to sea level. Moreover, the wind velocity at the particular geographical point was in the range of 3 to 4 meters per second. Wind speed was also measured using an anemometer positioned at a vertical distance of 30 meters to obtain data for a complete annual cycle. Previous studies recognized the significance of determining wind locations (Ahmad *et al.,* 2018) and this led to the observation of the parameter for 24 hours with data averaging intervals ranging from 15 minutes to 1 hour to collect wind profile data for an entire year. The records showed instances where the wind speed was lower than the mean value and the information obtained led to the modification within the HOMER software to account for probable losses.

The wind generator used in this study has a capacity of 5 kW and is specifically designed for the wind speed and load conditions at the BTP. It is equipped with a cut-in speed of 2.5 m/s, a rated speed of 17 m/s, a rotor consisting of three blades with a diameter of 5.0 meters, and a brushless permanent magnet

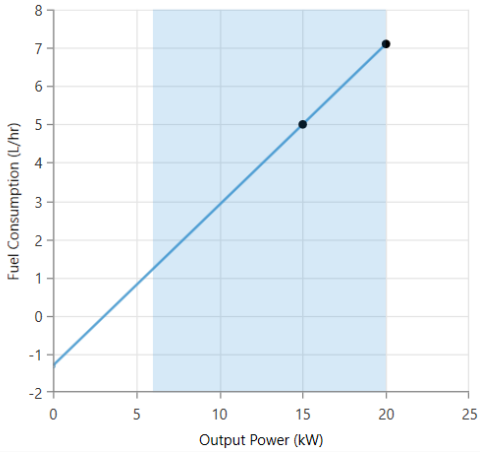

Fig 10 Diesel fuel consumption rate.

generator of the 9-pole type. The generator operates within an RPM range of 120 to 450 while the integration of wind energy as a power source into the hybrid inverter system led to the production of a direct current (DC) electrical output.

The diesel generator at the BTP provided the main power at 25 kVa/ 20 kW for SWRO and BWRO and was included in the optimization design. The fuel consumption curve of the generator for electricity generation is presented in Figure 10 based on a diesel density of 820 kg/m³ and a lower heating value of 43.2 MJ/kg. The fuel consumption rate was found to be 5 liters per hour (L/H) when the load was at 75% and increased to 7.1 L/H when the load reached 100%.

A minimum load ratio of 30% was recommended to be included in the simulation as a precaution against problems such as engine piston issues, cylinder leaks, and fires that could start when unburned fuel accumulated in the exhaust. This was intended to keep the diesel generator from running at very low levels for too long (Mathieu Lambert, 2023).

3) Optimization of DG Operational Scheduling

The optimization process focused on combining the existing system consisting of PV panels and BESS with other power sources such as WG and DG. The combination was regarded as the foundational system for the BTP. It was observed that the existing PV system had a total capacity of 36 kWp distributed equally across 3 individual strings. The PV system later served as a limiting factor for the 12 kWp, 24 kWp, and 36 kWp setups.

In this case, DG was used to reduce the number of times the microgrid network would experience load shedding by acting as a backup generator. Meanwhile, the fuel usage was minimized through the allocation of the base load to the specific

Table 6
Diesel Generator Operational Scenarios.

Scenario	DG Operating Time
Case 1	On 24 hours
Case 2	6.00 p.m. until 06.00 a.m.
Case 3	00.00 a.m. until 06.00 a.m.
Case 4	6.00 p.m. until 00.00 a.m.
Case 5	6.00 p.m. until 9.00 p.m.
Case 6	Off 24 hours

location of the microgrid (Mathieu Lambert, 2023) and the utilization of a "wound rotor synchronous generator (WRSG)" (Greig & Wang, 2017). Renewable energy sources and batteries were also implemented to effectively decrease the operational duration of DG in some isolated regions (Nejabatkhah, 2018). Another potential strategy was to modify the operational duration of DG within a hybrid off-grid system (Prawitasari, 2022) to ensure cost-effectiveness and improve the dependability of the microgrid system. This study organized the functioning of the DG into six separate scenarios as presented in the following Table 6.

4) Benefit-Cost Ratio Optimization

Benefit-cost ratio (BCR) analysis was conducted to determine the ideal layout of the microgrid system with due consideration for both economic and environmental advantages. BCR is a quantitative approach normally used to assess the economic viability of a project by examining the relationship between the benefits and expenses (Frej *et al.,* 2021; Roark *et al*., 2017). It was applied to consider and convert the anticipated benefits and costs associated with microgrid systems into present values (Kwak *et al.,* 2022). Some of the factors considered included enhanced reliability, energy conservation, decreased consumption, pollution mitigation, and savings in transmission system investment. (Chen *et al.,* 2018; Dwivedi *et al.,* 2022; Jin, 2015; Liang *et al.,* 2011; Yeo *et al.,* 2019). BCR analysis was conducted in this study using the following Equation 4:

$$BCR = \frac{C_{benefit}}{C_{ann}} \quad (4)$$

The criteria used to evaluate the advantages as follows:

1. CO_2 saving (pCO_2): The economic value of the carbon dioxide (CO_2) emissions mitigated through the utilization of energy derived from renewable sources was determined using Equation 5. The emission factor value was set at 0.53 kg/kWh (HOMER) and the carbon tax rate was \$0,0019/kg. (Direktorat Jenderal Pajak, 2022).

$$p_{CO2} = E_{supply} \times f_{emission} \quad (5)$$

In this context, E_{supply} represents the energy supply derived from renewable sources, measured in kilowatt-hours (kWh). Meanwhile, $f_{emission}$ refers to the emission factor, which quantifies the number of emissions produced per kilowatt-hour (kg/kWh). Lastly, carbon tax reflects the monetary value assigned to each kilogram of carbon emissions (\$/kg).

2. A Renewable Energy Certificate (REC) is a market-based mechanism that certifies the use of one MWh (megawatt-hour) of electricity from renewable sources by a holder. One Renewable Energy Certificate (REC) equals one megawatt-hour (MWh) of electrical energy produced from renewable energy sources and is valued at \$2,23 per megawatt-hour in dollars (PLN, 2021). The formula used to calculate REC in this study is presented in the following Equation 6.

$$REC = E_{supply} \times C_{REC} \quad (6)$$

In the given context, C_{REC} is the price of REC.

3. The percentage of the total generation cost determines the potential revenue from the energy output of the microgrid system, known as served energy. A positive correlation exists between the proportion of energy utilized and the potential revenue acquired. Conversely, the corresponding benefit diminishes as the amount of wasted energy increases.

$$p_{Ra} = (100\% - E_{excess}) \times C_{ann} \quad (7)$$

In this context, p_{Ra} represents the prospective income generated from energy consumption, E_{excess} is the surplus power, and C_{ann} signifies the annual cost. Equation 8 describes the total C_{ann} of a microgrid system consisting of all expenses associated with generating a specific amount of energy based on the production capacity.

$$C_{ann} = C_{losses} + C_{served} \quad (8)$$

C_{losses} represents the cost associated with energy losses while C_{served} denotes the cost of energy supplied. Therefore, BCR was computed using the following mathematical expression:

$$BCR = \frac{p_{CO2} + REC + p_R}{C_{ann}} \quad (9)$$

3. Results and Discussion

The optimization simulation produced results for the 167 system configurations evaluated based on excess energy, RF, LCOE, and BCR metrics. The selected baseline system served as a benchmark to identify the control and energy source configurations to be used as the foundation for the proposed system. The objective was to enhance the utilization of existing energy sources in the specific context of the BTP.

3.1 Load Impact Analysis

The simulation results for a 36 kWp PV generator with a focus on the BESS, WG, and DG from Case 1 to Case 6 scenarios are presented in the following Fig. It was observed that Load C could only be supplied by Case 1 where DG was on standby for 24 hours. However, Case 1 with CC dispatch strategy was unable to supply Loads A and B but all the loads were supplied with LF and CD strategies. The results showed that LF had better results for excess energy, renewable fraction (RF), LCOE, and BCR. This led to the conclusion that Case 1 with LF dispatch strategy was the best for a 36 kWp PV generator. The LF dispatch was used to optimize the energy generated by the New Renewable Energy (NRE) plant. The strategy only allowed the BESS to be charged through the excess power produced by NRE, such as PV systems, and prevented DG from charging the batteries. This showed that the DG was only used to generate power to satisfy unmet loads (Jufri *et al*., 2021b). Similar results were reported in hybrid generator simulations conducted in previous studies using PV, WG, BESS, and DG generators (Fatin Ishraque *et al.,* 2021; Manoj Kumar *et al*., 2020a; Shezan *et al.,* 2021)

The technical aspect of the analysis is presented in the graphs of Figure 11(a) and (b). It was observed from Fig 11(a) that the excess energy for Case 1 with LF dispatch was very high, reaching 56% when supplying Load A but the value reduced to 43% for larger Load B, and then to 22% for the most significant Load C. Moreover, the RF value was observed in Fig 11(b) to be increasing when Loads A, B, and C were supplied in succession. The trend showed that an increase in the load led to an increment in the RF value which was recorded to be 25% at Load A, then 42% at Load B, and reached 51% at Load C due to the incorporation of the surplus energy from NRE generators

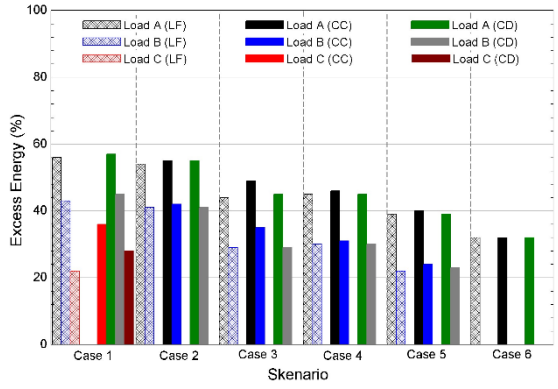

(a)

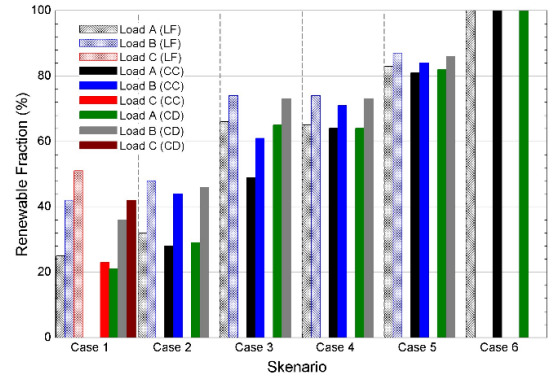

(b)

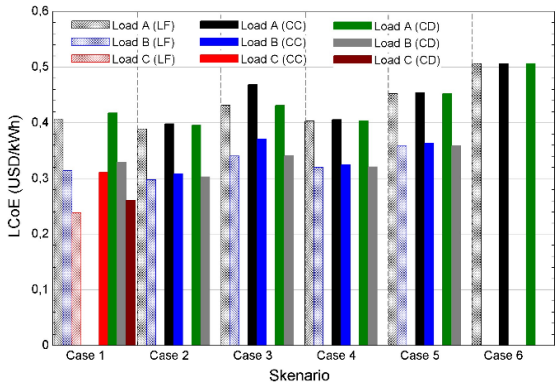

(c)

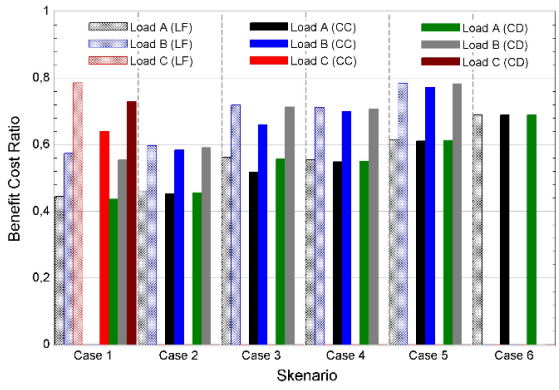

(d)

Fig 11. Graph of load variation against the parameters: (a) excess energy (b) RF (c) LCOE (d) BCR.

into the excess energy. The remaining energy from the NRE was partly used to supply the additional load. Technically, the system performed best when Case 1 with LF dispatch supplied Load C.

A similar study optimized the combination of 40.3 kWp PV, 3 kW WG, 23 kW DG, and 186-string BESS leading to the generation of an energy output of 87,438 kWh/year with an RF of 80.1%. However, some of the energy was not absorbed by the load and this led to a surplus of 18,976 kWh/year which was 21.7% of the total (Manoj Kumar *et al.*, 2020b). The percentage was close to the value recorded in this study when the system was connected to Load C. However, the RF was more significant than the value recorded in the previous study.

The economic aspect of the analysis is presented in the graphs of Figure 11 (c) and (d). The energy generation cost for Case 1 with LF was the highest when the system supplied Load A as observed in the $0.407/kWh recorded. The value reduced to $0.315/ kWh for Load B and the lowest was $0.238/kWh for Load C. Meanwhile, the LCOE reported in a previous study on PV/DG/WR/BESS configuration was $0.4382/kWh (Manoj Kumar et al., 2020b). BCR analysis in Fig(d) also showed that BCR value increased in sequence when supplying Loads A, B, and C with 0.445, 0.574, and 0.786 respectively. The criteria used to determine a good economic aspect was having the lowest possible production cost and a high benefit ratio. The results showed that Case 1 with LF dispatch had the best economic aspect. Therefore, it was concluded that the case was the best both technically and economically when connected to load C.

3.2 Analysis of the impact of power generation source configuration

The analysis was used to determine the impact of generator configuration on excess energy, RF, LCOE, and BCR within three distinct load scenarios. LF was used as the control dispatch because it was the optimal strategy based on the results from the previous analysis. The results presented in Fig showed that the addition of 36 kWp and 24 kWp PV systems with constant WG and DG in load A led to a 3-6% reduction in RF, a 14-25% decrease in excess energy, an 11-13% increase in BCR, and a 0.01 to 0.02 USD/kWh reduction in LCOE. Moreover, the absence of DG in Load A led to the production of the highest LCOE value which was recorded to be 0.51 USD/kWh with WG and 0.56 USD/kWh without WG, and RF was recorded to be 100%. These simulation results were observed to be in line with the reports of a previous study (Manoj Kumar *et al.*, 2020a). The trend showed that the highest values of BCR and excess energy were recorded in Load A. Furthermore, Load B had additional loads in the form of BWRO and SWRO, leading to the addition of energy from 36 kWp and 24 kWp PV at constant WG and DG capacity. The configuration increased excess energy by 8–11% and caused a significant advancement in RF by 8–21% while BCR decreased by 7–11% and LCOE by 0.03 to 0.06 USD/kWh. The addition of energy from 36 kWp and 24 kWp PV with constant WG capacity in Load C also led to an increase in excess energy by 3-8% and a significant improvement in RF by 12–21% while BCR reduced by 2-8% and LCOE by 0.03 to 0.06 USD/kWh.

The analysis showed that the renewable energy sources with larger capacity in the microgrid system produced lower LCOE and BCR but higher RF and excess energy. In terms of optimization, the addition of loads was observed to be an excellent choice to reduce excess energy and increase RF penetration to the maximum. For example, the energy generated from renewable energy sources in Load C was absorbed to the maximum and this led to low excess energy, reaching 10%, and

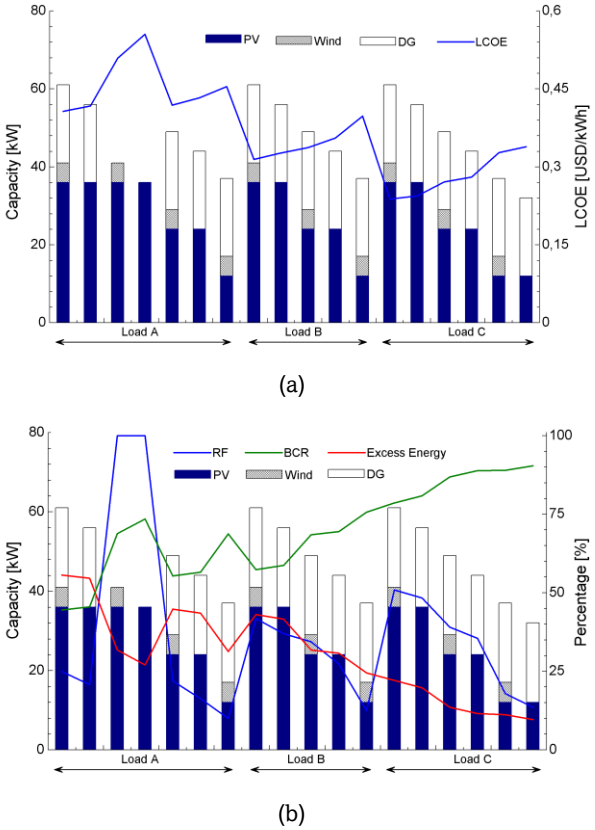

Fig 12. The influence of configuration variations on the parameters: (a) LCOE (b) RF, BCR, and excess energy.

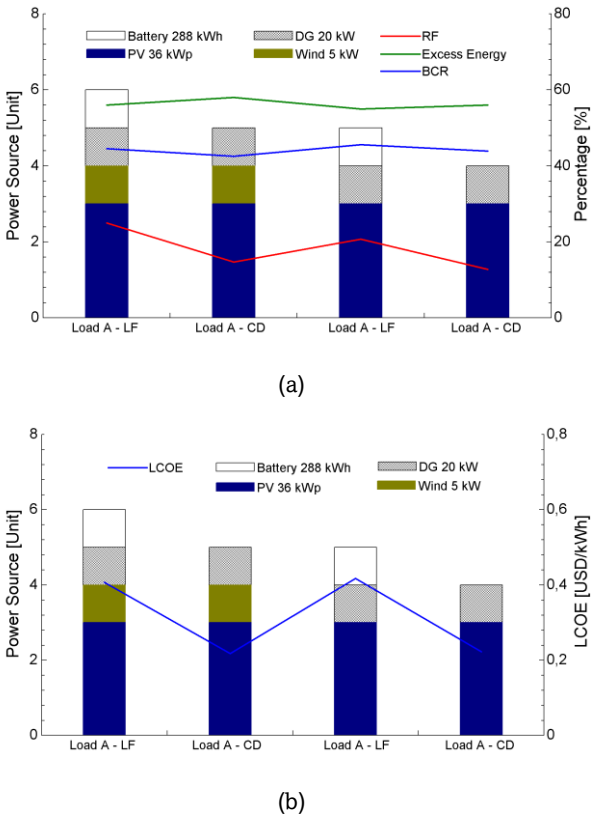

Fig 13. The influence of BESS configuration on excess energy, RF, BCR, and LCOE.

higher RF at 51%. The benefits were also recorded to be higher with a BCR value of 90% and LCOE at 0.24 USD/kWh.

BESS was applied in all the configurations presented in Figure 12 but the next analysis was focused on the systems without this energy source. The simulation results showed that the two control dispatches available in Load A were LF and CD as presented in Figure 13. BESS with LF was observed to have better RF, BCR, and excess energy than the other configurations. This was confirmed by the generation of 10% higher RF, 2% lower excess energy, and 2% higher BCR compared to the configuration with BESS. Meanwhile, the LCOE was 0.2 USD/kWh higher. The effectiveness of the renewable energy increased due to the storage in BESS which led to the reduction of excess energy while the increase in LCOE was influenced due to the capital and battery replacement costs.

3.3 Analysis of Diesel Generation Operational Impact

The system was designed with a 36 kWp PV, 5 kW WG, 20 kW DG, and a BESS with a storage capacity of 288 kWh. Moreover, Loads A, B, and C were managed using different control dispatch strategies. The operation of the DG was divided into six different scenarios, labeled as 1 to 6, as shown in Fig 14 (a) and (b). The results showed a positive correlation between the values of RF and excess energy with the change in the duration of DG operation as presented in Fig 14 (a). Meanwhile, the REC analysis in Fig 14 (b) showed that the BCR value had an upward trend as the duration of DG operation reduction for Loads A and B.

The study also focused on the level of LCOE in comparison to the baseline configuration based on the proposed configurations and scenarios. The results showed that an increase in the load size led to a decrease in the LCOE, as presented in Fig 14 (b). Moreover, the initial design, referred to as Case 1, used diesel and renewable energy sources to consistently fulfill the load requirements, and the operational duration was 12 hours higher than Case 2, leading to a higher LCOE value. This was assumed to be the reason for the augmented fuel consumption and operation and maintenance expenses of Case 1. Meanwhile, Case 2 was found to have the lowest LCOE value probably due to the operation duration of 12 hours, specifically from 18:00 to 6:00. DG was introduced when the alternative energy sources could not fulfill the prevailing demand. Therefore, the LCOE was evaluated when the diesel generator operated for six hours, specifically in Cases 3 and 4. The results showed that Case 4 had a comparatively lower value probably due to several active loads effectively harnessing the energy generated which led to a more comprehensive energy utilization. It was also observed that Cases 5 and 6 had the highest LCOE due to the increased capacity of renewable energy produced and stored in the BESS, leading to reduced DG utilization. Fig 15 further shows that Cases 1 and 2 had higher operational and fuel costs than other scenarios because DG was used for extended periods.

Cases 1 and 2 had lower replacement prices compared to 5 and 6 which required limited operational duration or complete non-functionality of the DG. This was due to the replacement and maintenance of degraded batteries and renewable energy sources integrated in these latter cases to ensure dependability. The DG system operated for six hours in Cases 3 and 4 but at different times compared to 1 and 2, leading to a reduction in the O&M and fuel costs. It was also observed that Cases 3 and

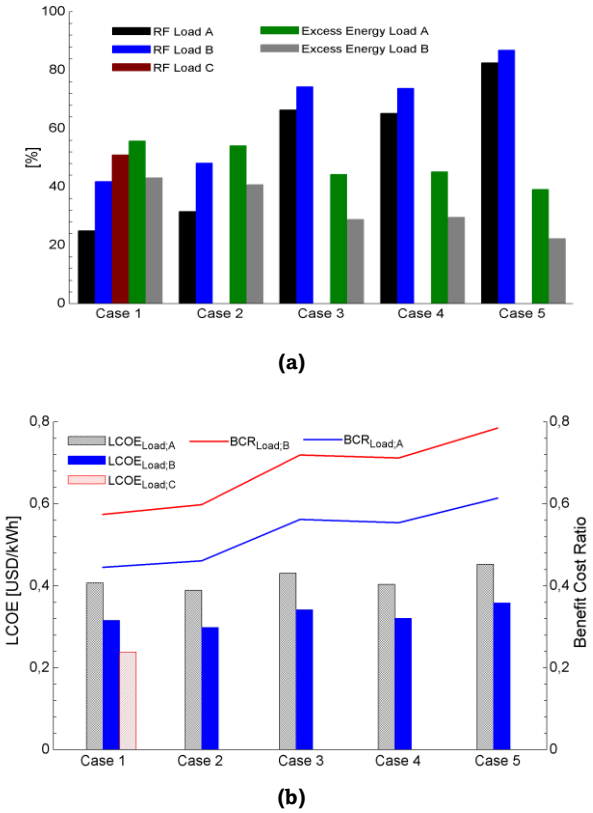

Fig 14(a) The influence of DG operational scenarios on excess energy and RF. (b) LCOE and BCR based on LF control dispatch.

4 had higher replacement costs compared to 1 and 2. This showed that the implementation of control techniques (Jufri *et al.,* 2021a) and optimization of the diesel generator scheduling could influence BESS performance and cycle lifespan (Amini *et al*, 2023).

3.4 Analysis of Optimal System Selection

Several systems were compared based on cost, efficiency, and renewable energy integration to determine the optimal solution as presented in Table 7 and Fig 16. The incorporation of Load B, a 36 kW PV system, WG, BESS, and DG operation from 6:00 p.m. to 6:00 a.m in System 1 led to minimal NPC expenses. Moreover, the reduction of DG operational hours to 6:00 p.m. - 9:00 p.m. while maintaining the same configuration in System 3 led to the maximization of RF with higher NPC and LCOE costs compared to System 1. The rationale behind the trend was the reduction in the operational hours of DG which caused a greater strain on the battery, potentially shortening the lifespan. This was in line with the findings of Gupta *et al.* (2021) and Zhou & Howey (2022) that the cycles of charging and discharging contributed to the degradation of battery life, causing the need for early replacement (Hosen *et al.,* 2021). Therefore, the system recommended to satisfy the minimum LCOE required was the combination of additional loads such as Load C as well as wind and diesel generators (DG) operating around the clock as proposed in System 2. This was due to the ability of the system to reduce energy losses from load integration and the utilization of WG and DG to reduce battery replacement expenses.

Energy losses can also be reduced by reducing the PV capacity and eliminating WG, as proposed in System 4. However, this adjustment led to an increased NPC and LCOE due to heightened operational and maintenance costs associated with the use of DG and batteries. A comparative analysis of the costs for each recommended system is provided in Fig 17.

The analysis of each optimization criterion showed different optimal system configurations but the recommendation from all was to incorporate a diesel generator and a larger load compared to the existing system. Moreover, the most optimal system was determined through the maximum BCR value which was obtained by comparing the energy and cost-saving abilities in Fig 18.

Figure 18 shows that the proposed system 1 with the minimum NPC Cost, proposed system 2 with the minimum LCOE, and proposed system 3 with maximum RF have superior cost and energy efficiency compared to both the existing and baseline systems. However, these systems were not as effective as the Proposed System 4 with the lowest excess energy due to the possibility of increased losses which could indirectly reduce energy efficiency and escalate energy costs. It is widely acknowledged that configuring and sizing the microgrid system in accordance with load requirements is important to ensure efficient resource utilization, cost minimization, and emission reduction (Ibrahim *et al.,* 2023; Meng *et al*., 2022).

The most optimal microgrid system recommended for the BTP Yogyakarta based on both energy and cost savings was the configuration with load C, a reduction in PV capacity by 24 kWp, absence of a wind turbine, 288 kWh battery storage, LF dispatch controller, and continuous DG operation. This was due to the ability of the system to produce an excess energy value of 12%, RF of 36%, CO_2 emission savings of 13.25 tons CO_2/year, LCOE of 28 cents/kWh, and BCR value of 0.89. The relatively low BCR value (<1) reflected limited economic viability in rural areas, mainly associated with high battery costs and modest economic value of carbon savings.

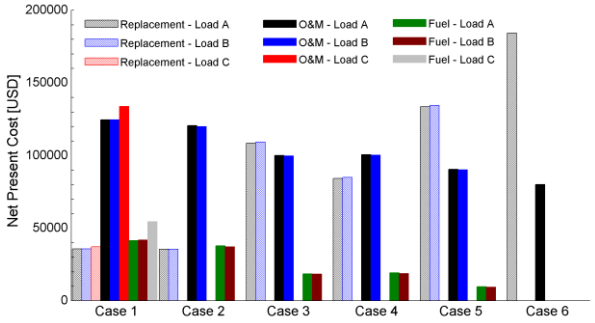

Fig 15. NPC classifies by cost category for LF control dispatch

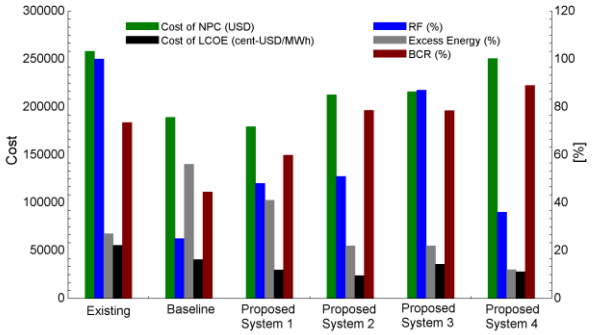

Fig 16 Multi-criteria comparison of the systems.

Table 7
Proposed system based on each criterion.

Optimization Criteria	System Configuration	Cost NPC ($)	LCOE (cent$/kWh)	RF (%)	Excess energy (%)	BCR
Existing	Load A/PV 36/BESS	258,047	55.5	100	27	0.735
Baseline	Load A/PV36/BESS/WG/DG 24hr	189,027	40.7	25	56	0.445
Proposed System 1 (Criteria 1)	Load B/PV36/WG/BESS/ DG (18.00-06.00)	**179,312**	29.8	48	41	0.598
Proposed System 2 (Criteria 2)	Load C/PV 36/BESS/WG/DG 24hr	212,729	23.8	51	22	0.786
Proposed System 3 (Criteria 3)	Load B/PV36/WG/BESS/ DG (18.00-21.00)	215,801	35.8	87	22	0.785
Proposed System 4 (Criteria 4)	Load C/PV24/BESS/DG 24hr	250,478	28.0	36	12	0.889
Proposed System 4 (Criteria 5)	Load C/PV24/BESS/DG 24hr	250,478	28.0	36	12	0.889

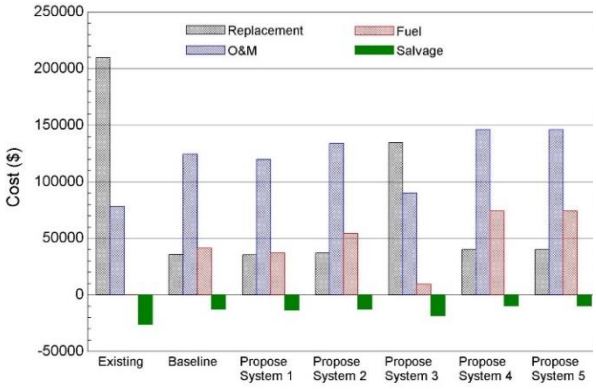

Fig 17. Replacement, O&M, fuel, and salvage cost comparison.

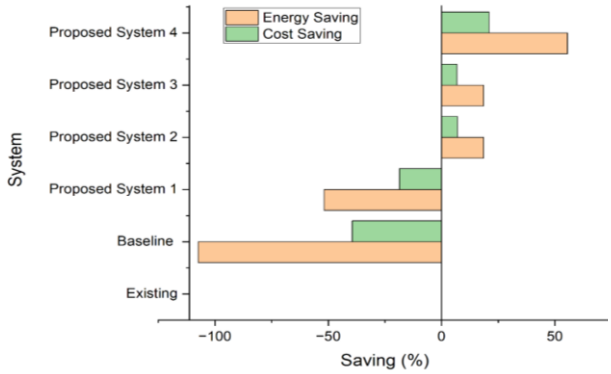

Fig 18. Energy and cost-saving comparison

The proposed system had energy and cost savings of 55.56% and 20.95% respectively compared to the existing system without DG. This was due to the optimization of the generation and load system configuration to minimize energy losses. Moreover, the replacement of batteries with DG to fulfill load requirements during specific periods could prolong battery lifespan and reduce replacement expenses, indirectly contributing to overall cost savings.

4. Conclusion

In conclusion, this study was aimed to optimize the existing microgrid system in "3T" areas to ensure improved sustainability and economic viability. This was achieved by proposing a decision-making process to systematically analyze and evaluate different microgrid configurations by considering daily load profile variations, control dispatch algorithm selection, power supply system reconfiguration, and diesel generator operation scheduling. Moreover, the optimal systems were later selected based on the optimization objective criteria including minimum NPC, minimum LCOE, maximum RF, minimum excess energy, and maximum BCR.

The results showed that all the criteria recommended the introduction of diesel generators (DG) and greater loads to the microgrid system in BTP. The optimal system with the maximum BCR was later achieved with the inclusion of additional loads, reduction of PV capacity, battery storage, LF controller, and DG operation for 24 hours a day. This led to a 55% increase in energy efficiency and 20.95% in cost savings compared to the existing system without DG.

Despite these benefits, the economic feasibility of microgrid systems in rural areas remains limited due to high battery costs and low carbon-saving economic value. Therefore, developing affordable alternative energy storage solutions and implementing a profitable carbon pricing strategy are critical to improving the sustainability and economics of these systems, particularly in rural areas. Future studies can focus on developing tailored predictive control systems specifically designed according to local conditions to enhance the durability and economic viability of batteries. Moreover, machine learning algorithms can also be investigated to drive further advancements in order to establish a more promising and environmentally friendly future for remote communities.

Acknowledgment

The authors would like to acknowledge Andri Subandriya, Ahmad Gusyairi, and Munadiyan Nurhuda for their contributions to the BTP project and data.

Funding

This study was financially supported in 2023 by the Renewable Energy Programme House, Research Organization on Energy and Manufacturing, under National Research and Innovation (BRIN), Indonesia.

Conflicts of Interest

The authors declare no conflicts of interest.

References

Ahmad, J., Imran, M., Khalid, A., Iqbal, W., Ashraf, S. R., Adnan, M., Ali, S. F., & Khokhar, K. S. (2018). Techno economic analysis of a wind-photovoltaic-biomass hybrid renewable energy system for rural electrification: A case study of Kallar Kahar. *Energy*, *148*, 208–234. https://doi.org/10.1016/j.energy.2018.01.133

Amini, M., Nazari, M.H., Hosseinian, S. H. (2023). Optimal energy management of battery with high wind energy penetration-A comprehensive linear battery degradation cost model. *Sustainable Cities and Society*, *93*. https://doi.org/10.1016/j.scs.2023.104492

Anglani, N., Oriti, G., & Colombini, M. (2017). Optimized energy management system to reduce fuel consumption in remote military microgrids. IEEE Transactions on Industry *Applications*, *53*(6), 5777–5785. https://doi.org/10.1109/TIA.2017.2734045

Azahra, A., Syahindra, K. D., Aryani, D. R., Jufri, F. H., & Ardita, I. M. (2020). Optimized configuration of photovoltaic and battery energy storage system (BESS) in an isolated grid: A case study of Eastern Indonesia. *IOP Conference Series: Earth and Environmental Science*, *599*(1). https://doi.org/10.1088/1755-1315/599/1/012017

Beza, T. M., Wu, C. H., & Kuo, C. C. (2021). Optimal sizing and techno-economic analysis of minigrid hybrid renewable energy system for tourist destination islands of lake tana, ethiopia. *Applied Sciences (Switzerland)*, *11*(15). https://doi.org/10.3390/app11157085

Bhamidi, L., & Sivasubramani, S. (2020). Optimal Planning and Operational Strategy of a Residential Microgrid with Demand Side Management. *IEEE Systems Journal*, *14*(2), 2624–2632. https://doi.org/10.1109/JSYST.2019.2918410

Çetinbaş, İ., Tamyürek, B., & Demirtaş, M. (2019). Design, analysis and optimization of a hybrid microgrid system using HOMER software: Eskişehir osmangazi university example. *International Journal of Renewable Energy Development*, *8*(1), 65–79. https://doi.org/10.14710/ijred.8.1.65-79

Chen, Q., Yuan, X., He, Y., Guo, L., Cai, Y., & Chen, Q. (2018). Investment and Optimization of Off-Grid Microgrid Projects Based on Life-Cycle Cost/Benefit Analysis With Open Investment Mode. *Dianwang Jishu/Power System Technology*, *42*(8), 2448–2455. https://doi.org/10.13335/j.1000-3673.pst.2017.2832

Chisale, S. W., Eliya, S., & Taulo, J. (2023). Optimization and design of hybrid power system using HOMER pro and integrated CRITIC-PROMETHEE II approaches. *Green Technologies and Sustainability*, *1*(1), 100005. https://doi.org/10.1016/j.grets.2022.100005

Dahiru, A. T., & Tan, C. W. (2020). Optimal sizing and techno-economic analysis of grid-connected nanogrid for tropical climates of the Savannah. *Sustainable Cities and Society*, *52*. https://doi.org/10.1016/j.scs.2019.101824

Dei, T., & Batjargal, N. (2022). Technical and Economical Evaluation of Micro-Solar PV/Diesel Hybrid Generation System for Small Demand. *International Journal of Renewable Energy Development*, *11*(4), 1101–1112. https://doi.org/10.14710/ijred.2022.46747

Díaz-Bello, D., Vargas-Salgado, C., Águila-León, J., & Lara-Vargas, F. (2023). Methodology to Estimate the Impact of the DC to AC Power Ratio, Azimuth, and Slope on Clipping Losses of Solar Photovoltaic Inverters: Application to a PV System Located in Valencia Spain. *Sustainability (Switzerland)*, *15*(3). https://doi.org/10.3390/su15032797

Direktorat Jenderal Pajak. (2022). Undang-undang harmonisasi peraturan perpajakan. https://www.pajak.go.id/sites/default/files/2021-12/Paparan%20Sosialisasi%20%20UU%20HPP%202021_0.pdf

Direktorat Jenderal Pengendalian Perubahan Iklim. (2017). *STRATEGI IMPLEMENTASI NDC*. https://ditjenppi.menlhk.go.id/reddplus/images/adminppi/dokumen/strategi_implementasi_ndc.pdf

Dirjen Ketenagalistrikan ESDM. (2023). Capaian subsektor ketenagalistrikan tahun 2022 dan program kerja tahun 2023. https://gatrik.esdm.go.id/assets/uploads/download_index/files/3b91e-30012023r3-tayang-bahan-konfrensi-pers-gatrk.pdf

Dwivedi, D., Babu, K. V. S. M., Yemula, P. K., Chakraborty, P., & Pal, M. (2022). *Evaluation of Energy Resilience and Cost Benefit in Microgrid with Peer-to-Peer Energy Trading*. http://arxiv.org/abs/2212.02318

Emetere, M. E., & Akinyemi, M. L. (2015). Weather Effect on Photovoltaic Module Adaptation in Coastal Areas. *International Journal of Renewable Energy Research*, *5*(3), 821–825. https://doi.org/10.20508/ijrer.v5i3.2418.g6645

Emetere, M. E., Akinyemi, M. L., & Edeghe, E. B. (2016). A Simple Technique for Sustaining Solar Energy Production in Active Convective Coastal Regions. *International Journal of Photoenergy*, *2016*, 1–11. https://doi.org/10.1155/2016/3567502

Fatin Ishraque, M., Shezan, S. A., Ali, M. M., & Rashid, M. M. (2021). Optimization of load dispatch strategies for an islanded microgrid connected with renewable energy sources. *Applied Energy*, *292*, 1–19. https://doi.org/10.1016/j.apenergy.2021.116879

Frej, E. A., Ekel, P., & de Almeida, A. T. (2021). A benefit-to-cost ratio based approach for portfolio selection under multiple criteria with incomplete preference information. *Information Sciences*, *545*, 487–498. https://doi.org/10.1016/j.ins.2020.08.119

Greig, M., & Wang, J. (2017). Fuel Consumption Minimization of Variable-Speed Wound Rotor Diesel Generators. *IECON 2017 - 43rd Annual Conference of the IEEE Industrial Electronics Society*. https://doi.org/10.1109/IECON.2017.8217506

Gupta, M., Mary, S., Trivedi, J., Goyal, J., Maan, P., & Singh, M. (2021). *Battery Lifetime Estimation Based on Usage Pattern* (pp. 353–365). https://doi.org/10.1007/978-981-16-2709-5_27

Hosen, M. S., Youssef, R., Kalogiannis, T., Van Mierlo, J., & Berecibar, M. (2021). Battery cycle life study through relaxation and forecasting the lifetime via machine learning. *Journal of Energy Storage*, *40*, 102726. https://doi.org/10.1016/j.est.2021.102726

Hou, J., Yu, W., Xu, Z., Ge, Q., Li, Z., & Meng, Y. (2023). Multi-time scale optimization scheduling of microgrid considering source and load uncertainty. *Electric Power Systems Research*, *216*, 109037. https://doi.org/10.1016/J.EPSR.2022.109037

Ibrahim, I. M., Abdelaziz, A. Y., Alhelou, H. H., & Omran, W. A. (2023). Sizing of Microgrid System Including Multi-Functional Battery Storage and Considering Uncertainties. *IEEE Access*, *11*, 29521–29540. https://doi.org/10.1109/ACCESS.2023.3259459

Intergovernmental Panel On Climate Change. (2006). V2_1_Ch1_Introduction 2006 IPCC Guidelines. *Intergovernmental Panel On Climate Change*, *2*(Energy). https://www.ipcc-nggip.iges.or.jp/public/2006gl/pdf/2_Volume2/V2_1_Ch1_Introduction.pdf

Ishraque, M. F., Shezan, S. A., Rashid, M. M., Bhadra, A. B., Hossain, M. A., Chakrabortty, R. K., Ryan, M. J., Fahim, S. R., Sarker, S. K., & Das, S. K. (2021). Techno-Economic and Power System Optimization of a Renewable Rich Islanded Microgrid Considering Different Dispatch Strategies. *IEEE Access*, *9*, 77325–77340. https://doi.org/10.1109/ACCESS.2021.3082538

Jahangir, M. H., Abdi, A., & Fakouriyan, S. (2023). Energy demand supply of small-scale medical centers in epidemic conditions of Covid-19 with hybrid renewable resources. *Energy Reports*, *9*, 5449–5457. https://doi.org/10.1016/J.EGYR.2023.04.362

Jin, X. (2015). Analysis of microgrid comprehensive benefits and evaluation of its economy. *IET Seminar Digest*, *2015*(8). https://doi.org/10.1049/ic.2015.0279

Jmii, H., Abbes, M., Meddeb, A., & Chebbi, S. (2020). Centralized VSM control of an AC meshed microgrid for ancillary services provision. *International Journal of Electrical Power & Energy Systems*, *115*, 105450. https://doi.org/10.1016/J.IJEPES.2019.105450

Jufri, F. H., Aryani, D. R., Garniwa, I., & Sudiarto, B. (2021a). Optimal battery energy storage dispatch strategy for small-scale isolated hybrid renewable energy system with different load profile patterns. *Energies*, *14*(11). https://doi.org/10.3390/en14113139

Jufri, F. H., Aryani, D. R., Garniwa, I., & Sudiarto, B. (2021b). Optimal battery energy storage dispatch strategy for small-scale isolated hybrid renewable energy system with different load profile patterns. *Energies*, *14*(11). https://doi.org/10.3390/en14113139

Kementerian Sekretariat negara Republik Indonesia. (2020). *Peraturan Presiden RI Nomor 63 Tahun 2O20*. https://jdih.setkab.go.id/PUUdoc/176108/Perpres_Nomor_63_Tahun_2020.pdf

Kemeterian Sekretariat Negara Republik Indonesia. (2020). *Perpes No 63 Tahun 2020 Tentang Penetapan Daerah Tertinggal Tahun 2020-2024*. https://peraturan.go.id/id/perpres-no-63-tahun-2020

Khamharnphol, R., Kamdar, I., Waewsak, J., Chaichan, W., Khunpetch, S., Chiwamongkhonkarn, S., Kongruang, C., & Gagnon, Y. (2023). Microgrid Hybrid Solar/Wind/Diesel and Battery Energy Storage Power Generation System: Application to Koh Samui, Southern Thailand. *International Journal of Renewable Energy Development*, *12*(2), 216–226. https://doi.org/10.14710/ijred.2023.47761

Kwak, Y.-G., Lee, B.-H., & Kang, F.-S. (2022). Economic Efficiency Analysis Based on Benefit-Cost Ratio of Floating Photovoltaic Power Generation System. *Transactions of the Korean Institute of Electrical Engineers*, *71*(8), 1117–1125. https://doi.org/10.5370/KIEE.2022.71.8.1117

Lambert, M. and Hassani, R. (2023). Diesel genset optimization in remote microgrids. *Applied Energy*, *340*. https://doi.org/10.1016/j.apenergy.2023.121036

Liang, H., Cheng, L., & Su, J. (2011). Cost benefit analysis for microgrid. *Zhongguo Dianji Gongcheng Xuebao/Proceedings of the Chinese Society of Electrical Engineering*, *31*(SUPPL. 1), 38–44.

Liu, X., & Liu, Y. (2019). Optimal planning of AC-DC hybrid transmission and distributed energy resource system: Review and prospects. *CSEE Journal of Power and Energy Systems*. https://doi.org/10.17775/CSEEJPES.2019.00540

Manoj Kumar, N., Chopra, S. S., Chand, A. A., Elavarasan, R. M., & Shafiullah, G. M. (2020a). Hybrid renewable energy microgrid for a residential community: A techno-economic and environmental perspective in the context of the SDG7. *Sustainability (Switzerland)*, *12*(10), 1–30. https://doi.org/10.3390/SU12103944

Martirano, L., Parise, G., Greco, G., Manganelli, M., Massarella, F., Cianfrini, M., Parise, L., Di Laura Frattura, P., & Habib, E. (2019). Aggregation of users in a residential/commercial building managed by a Building Energy Management System (BEMS). *IEEE Transactions on Industry Applications*, *55*(1), 26–34. https://doi.org/10.1109/TIA.2018.2866155

Meng, Z., Meng, L., Wang, L., Zhou, H., & Hu, X. (2022). Research on Equipment Configuration and Operation Optimization of Microgrid System. *2022 4th Asia Energy and Electrical Engineering Symposium (AEEES)*, 138–141. https://doi.org/10.1109/AEEES54426.2022.9759791

Mudaheranwa, E., Ntagwirumugara, E., Masengo, G., & Cipcigan, L. (2023). Microgrid design for disadvantaged people living in remote areas as tool in speeding up electricity access in Rwanda. *Energy Strategy Reviews*, *46*. https://doi.org/10.1016/j.esr.2023.101054

Nejabatkhah, F. (2018). Optimal Design and Operation of a Remote Hybrid Microgrid. *CPSS Transactions on Power Electronics and Applications*, *3*(1), 3–13. https://doi.org/10.24295/CPSSTPEA.2018.00001

PLN. (2021). *Renewable Energy Certificate (REC)*. https://layanan.pln.co.id/renewable-energy-certificate/informasi

Prawitasari, A. (2022). *Optimasi Sistem Operasi Pembangkit Hibrida Dengan Pemodelan Profil Beban Di Daerah 3T*. https://doi.org/https://doi.org/10.36418/syntax-literate.v7i5.7074

PT PLN. (2021). *Rencana Usaha Penyediaan Tenaga Listrik (RUPTL) PT PLN Tahun 2021-2030*. https://gatrik.esdm.go.id/assets/uploads/download_index/files/38622-ruptl-pln-2021-2030.pdf

Roark, J., Weng, D., & Maitra, A. (2017). Measuring the value of microgrids: a benefit-cost framework. *CIRED - Open Access Proceedings Journal*, *2017*(1), 1992–1994. https://doi.org/10.1049/oap-cired.2017.1324

See, A. M. K., Mehranzamir, K., Rezania, S., Rahimi, N., Afrouzi, H. N., & Hassan, A. (2022). Techno-economic analysis of an off-grid hybrid system for a remote island in Malaysia: Malawali island, Sabah. *Renewable and Sustainable Energy Transition*, *2*, 100040. https://doi.org/10.1016/j.rset.2022.100040

Shezan, S. A., Hasan, K. N., Rahman, A., Datta, M., & Datta, U. (2021). Selection of appropriate dispatch strategies for effective planning and operation of a microgrid. *Energies*, *14*(21), 1–19. https://doi.org/10.3390/en14217217

Sulistyo, I. T., & Far, A. J. (2020). Design and analysis of a smart microgrid for a small island in Indonesia. *International Journal of Smart Grid and Clean Energy*, 967–974. https://doi.org/10.12720/sgce.9.6.967-974

Thirugnanam, K., Kerk, S. K., Yuen, C., Liu, N., & Zhang, M. (2018). Energy Management for Renewable Microgrid in Reducing Diesel Generators Usage with Multiple Types of Battery. *IEEE Transactions on Industrial Electronics*, *65*(8), 6772–6786. https://doi.org/10.1109/TIE.2018.2795585

Upadhyay, S., & Sharma, M. P. (2016). Selection of a suitable energy management strategy for a hybrid energy system in a remote rural area of India. *Energy*, *94*, 352–366. https://doi.org/10.1016/j.energy.2015.10.134

Yaouba, Z., Falama, R., Ngangoum Welaji, F., Hamda Soulouknga, M., Kwefeu Mbakop, F., & Dadjé, A. (2022). Optimal Decision-Making on Hybrid Off-Grid Energy Systems for Rural and Remote Areas Electrification in the Northern Cameroon. *Journal of Electrical and Computer Engineering*, *2022*. https://doi.org/10.1155/2022/5316520

Yeo, S.-H., Lee, W.-H., Kim, C.-S., Park, S.-M., & Ko, J.-H. (2019). Economic analysis of industrial complex microgrid (MG)with six factories. *International Journal of Advanced Science and Technology*, *28*(5), 111–120. https://www.scopus.com/inward/record.uri?eid=2-s2.0-85080127757&partnerID=40&md5=4f21fc4cc13a05a02f574fe527151773

Zhou, Z., & Howey, D. A. (2022). Bayesian hierarchical modelling for battery lifetime early prediction. IFAC-PapersOnLine. 56(2), 6117-6123. https://doi.org/10.1016/j.ifacol.2023.10.708